Original Papers

Two-dimensional Observation of Emission Spectra Excited from Laser Induced Plasmas and the Application to Emission Spectrometric Analysis

Chizuru KITAOKA and Kazuaki WAGATSUMA†

Institute for Materials Research, Tohoku University, 2-1-1 Katahira, Sendai 980–8577, Japan

The spatial distribution analysis of emission signals from a laser-induced plasma can provide information on the excitation mechanism as well as on the optimization of the analytical conditions when it is employed as a sampling and excitation source in optical emission spectrometry. A two-dimensionally imaging spectrometer system was employed to measure spatial variations in the emission intensities of a copper sample and plasma gases when krypton, argon, or helium was employed under various pressure conditions. The emission image of the Cu I 324.75-nm line consists of a breakdown spot and a plasma plume, where the breakdown zone expands toward the surrounding gas. The shape and the intensities of the plasma plume are strongly dependent on the kind and pressure of the plasma gas, while those of the breakdown zone are less influenced by these experimental parameters. This effect can be explained by the difference in the cross-section of collisions between krypton, argon, and helium. The signal-to-background ratio of the Cu I 324.75-nm line was estimated over two-dimensional images to determine the optimum position for analytical applications.

(Received July 26, 2007; Accepted September 3, 2007; Published November 10, 2007)

Introduction

Laser-induced plasma spectrometry (LIPS) is a powerful technique for the direct analysis of various materials because of a rapid response without any sample pretreatment.[1] A Q-switched Nd:YAG laser, which is irradiated onto a sample surface during a very short period but with a large power density, produces a pulsated laser-induced plasma (LIP) at the repetition frequency of the laser. Sample atoms are ejected from the surface due to laser ablation and are subsequently ionized and excited in LIP; therefore, the LIP acts as an excitation source as well as a sampling source to give a simple analytical method for atomic emission spectrometry. It is thus expected that LIPS can be employed for on-line/on-site process control in various industries.[2]

The pulsated LIP has both spatial and temporal variations, depending on various experimental parameters, such as the kind and pressure of the plasma gas employed, which is generally known as an expansion process of the plasma. Previous papers are reported that the emission zone varied with the progress of the plasma to produce a plume-like shape, which was strongly dependent on the nature of the plasma gas.[3–6] Time-resolved measurements of the emission spectra give useful information on optimization of the experimental conditions in the emission spectrometric applications, such as the delay time as well as the gate width on the data acquisition;[7,8] however, they can not provide the overall variations of the plasma expansion. For this purpose, a two-dimensional (2D) image of a spectral line emitted from the LIP should be observed, which would yield information on the fundamental processes occurring in the LIP. Previous studies employed interference filters having bad spectral resolution of more than 10 nm; however, they were not suitable for measuring emission spectra comprising many spectral lines. Few studies regarding 2D spectral images have been published mainly due to a lack of spectrometers enabling 2D observations having good spectral resolution.

In this study, we investigated 2D images of several emission lines from reduced-pressure LIPs by using an imaging spectrograph equipped with a CCD detector, when krypton, argon, or helium was employed as the plasma gas. The excitations of the emission lines are discussed here based on the variations of the 2D images against the pressures of each plasma gas.

† To whom correspondence should be addressed.
E-mail: wagatuma@imr.tohoku.ac.jp

Experimental

A schematic diagram of the apparatus is shown in Fig. 1. A Nd:YAG laser (LOTIS T II U LS-2135, Japan) was employed at a wavelength of 532 nm (SHG mode). A laser energy of 40 mJ/pulse was set to obtain sufficient sample ablation. A pulse duration of about 10 ns and a repetition rate of 10 Hz were employed. A spherical lens with a 200-nm focal length was used to focus the laser beam onto the target surface. The energy of the pulsed laser was measured using a thermopile absorber and a laser power/energy monitor (OPHIR JAPAN 3A-P-CAL, NOVA, Japan).

High-purity argon (>99.99995%), krypton (>99.999%), or helium (>99.99999%) was introduced as the plasma gas after evacuating the chamber to below 7 Pa. The pressure was monitored with a Pirani gauge (GP-2, ULVAC Corp., Japan) and a capacitance manometer (MK 11B-2-P and 127AA-001003, NKS Instruments Inc., USA), which were placed between the evacuation port and rotary vacuum pump (GLD-166, ULVAC Engineering Inc., Japan). The plasma gas was

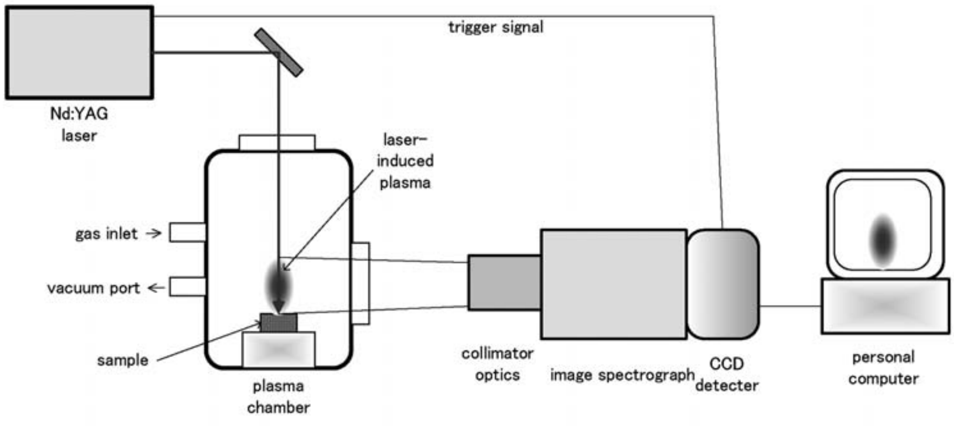

Fig. 1 Experimental setup.

flowed during the measurement while keeping the chamber pressure between 13×10^2 and 670×10^2 Pa.

Emission signals from the LIP were conducted through a collimator optics onto the entrance slit of an image spectrograph (Model 12580, BunkoKeiki Corp., Japan), and the emission image was then dispersed and detected on a charge-coupled device detector (SensiCam QE Model, PCO Imaging Corp., Germany), where the 2D image of a particular emission line could be observed. The spectral resolution was 0.1 – 2.0 nm, depending on the slit width.

High-purity copper plates (99.99%) were used as the sample. The sample plate was polished with water-proof abrasive papers and then fixed at the sample port of the chamber. After the surface was cleaned using the first 100 laser shots, the emission signal was averaged during the next 10 shots and stored in a personal computer. Each image was recorded for the period of 0.01 ms (gate width). The analytical lines were Cu I 324.75 nm (3.82 eV) for the sample, and Kr I 431.96 nm (12.78 eV), Ar I 420.07 nm (14.50 eV), and He I 388.86 nm (23.01 eV) for the plasma gases.[9–11]

Results and Discussion

2D image of copper emission line

Figure 2 shows 2D emission images of the Cu I 324.75-nm line and the background position measured at 315.0 nm, whose intensities are expressed by mapping with several colors, when krypton (a), argon (b), or helium (c) is introduced at various gas pressures. Their colored maps indicate that the images roughly comprise two portions: a narrow spot on the sample surface where the breakdown of LIP occurs and a portion expanding towards surrounding gas which is called a plasma plume. The size and the intensities of the plasma plume are largely dependent on the kind as well as the pressure of the plasma gas, whereas those of the breakdown spot are less influenced by these experimental parameters. The breakdown spots are clearly found not only at the wavelength of the Cu I line but at the background position, regardless of the experimental conditions; however, the background emission is drastically reduced as the plume expands away from the breakdown zone. In the region of the plasma plume, the Cu I intensity emitted from the helium LIP can be observed only at the large gas pressures of 400×10^2 and 670×10^2 Pa, which is much less intense compared to the argon and the krypton LIPs. It is further found that the Cu I intensities from the plasma plume generally become larger at higher gas pressures in all cases of the plasma gases, and that the emission area of the argon LIP is more expanded than that of the krypton LIP which gives larger Cu I emission intensities. The emission images in Figs. 2(a) and (b) also indicate that the bright emission area of the Cu I line is more concentrated at higher gas pressures in the krypton LIP rather than the argon LIP. The most intense emission zone of the Cu I line was obtained when krypton gas was employed at the pressure of 670×10^2 Pa.

A hot breakdown zone is produced on a sample surface immediately after laser irradiation. Because of direct coupling with a pulsed laser having a very high power density, the sample material is ablated and then excited and ionized through various collisions among highly-energetic particles in the breakdown zone, where electrons, ions, and atoms having large kinetic energies are produced and then they move towards the surrounding gas. The following reactions represent the processes occurring in the breakdown zone:

$$\begin{aligned}&\text{Cu (fast)} \longrightarrow \text{Cu}^+ + \text{e}^- \text{(fast)} \longrightarrow \text{Cu}^{z+} + z\text{e}^- \text{(fast)},\\&\text{G (fast)} \longrightarrow \text{G}^+ + \text{e}^- \text{(fast)} \longrightarrow \text{G}^{z+} + z\text{e}^- \text{(fast)},\end{aligned} \quad (1)$$

where G is an atom of the plasma gas and the term, “fast”, means a particle having large kinetic energy. Also, various recombination reactions take place simultaneously, for example,

$$\begin{aligned}&\text{Cu}^+ + \text{e}^- \longrightarrow \text{Cu}^* + \Delta E,\\&\text{G}^+ + \text{e}^- \longrightarrow \text{G}^* + \Delta E.\end{aligned} \quad (2)$$

These reactions produce excited species of copper and plasma gas, denoted by Cu* and G*. The resulting excess energy, ΔE, is released through a continuum background over a wide wavelength range. The background emission, which is observed near the sample surface in Fig. 2, is derived principally from the recombination continuum.

On the other hand, excited species of copper and plasma gas are also produced through direct collisional excitations, for example,

$$\text{Cu} + \text{e}^- \text{(fast) or G (fast)} \longrightarrow \text{Cu}^* + \text{e}^- \text{(slow) or G (slow)}, \quad (3)$$

$$\text{G} + \text{e}^- \text{(fast) or G (fast)} \longrightarrow \text{G}^* + \text{e}^- \text{(slow) or G (slow)}. \quad (3')$$

The excited species resulting from the reactions (2) and (3) contribute to the characteristic emission lines in the spectrum emitted from the breakdown zone.

After the breakdown plasma zone expands upward, the

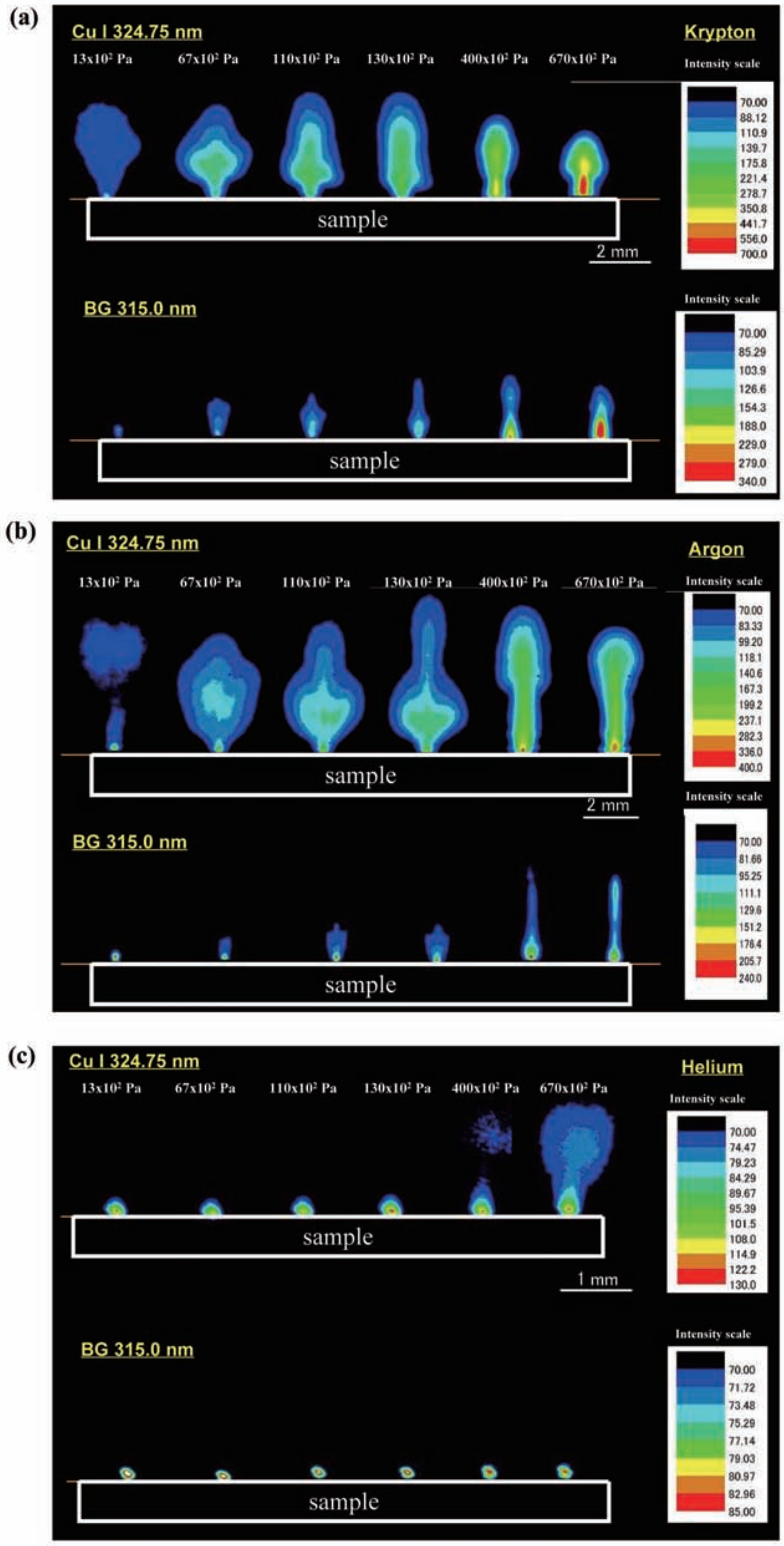

Fig. 2 Two-dimensional emission images of Cu I 324.75 nm and the background measured at 315.0 nm when krypton (a), argon (b), and helium (c) is employed as the plasma gas at pressures of 13×10^2, 67×10^2, 110×10^2, 130×10^2, 400×10^2, and 670×10^2 Pa.

characteristic of the resulting plasma plume largely varies due to the kind and pressure of the plasma gas. The number density of highly-energetic particles should decrease as the plasma plume expands more broadly. Especially, the number density of electrons is rapidly reduced due to recombination with charged particles (see Eq. (2)) because such collisions have very large cross-sections. Therefore, the recombination continuum would decrease rapidly with the progress of the plasma plume, which can explain the behavior of the background emission at 315.0 nm, as shown in Fig. 2. Also, the excitations through the first-

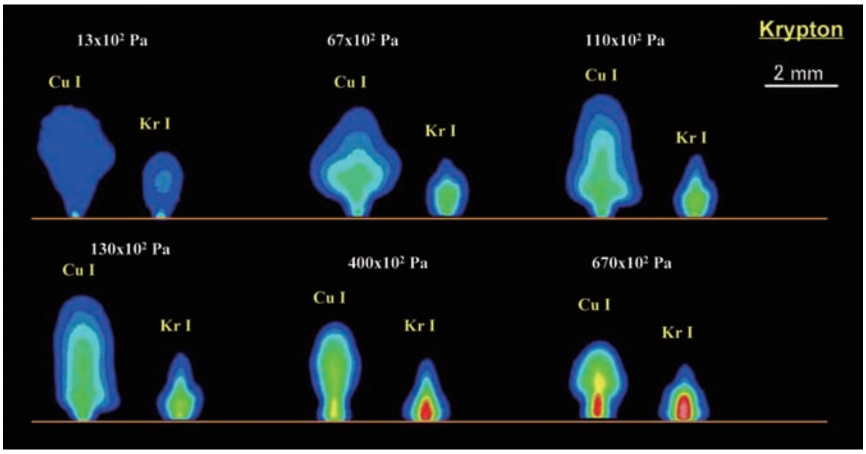

Fig. 3 Comparison in the 2D images between Cu I 324.75 nm and Kr I 431.96 nm at krypton pressures of 13×10^2, 67×10^2, 110×10^2, 130×10^2, 400×10^2, and 670×10^2 Pa.

kind collisions, as indicated in Eq. (3), take place less actively; however, some of the energetic particles still survive during the plasma expansion and provide their kinetic energies to excite copper and plasma gas atoms.

It is considered that the shape and the intensities of the plasma plume are determined through the interaction between energetic particles produced after the laser breakdown and the surrounding gas. Gas atoms having larger collisional cross-sections could receive the kinetic energy of these energetic particles more effectively, and then their energies could be consumed to excite copper and plasma gas atoms through subsequent collisions occurring in the plasma plume. Based on this criterion, krypton gas is expected to work as the most effective energy receiver, compared to argon and helium. In fact, the thermal conductivity for each plasma gas is as follows: 1.52×10^{-3} W cm^{-1} K^{-1} for helium, 1.77×10^{-4} W cm^{-1} K^{-1} for argon, and 9.45×10^{-5} W cm^{-1} K^{-1} for krypton, meaning that krypton can reserve energies the most effectively. The mean free path of atom-atom collision was reported to be 17.6×10^{-5} m for helium, 8.1×10^{-5} m for argon, and 6.6×10^{-5} m for krypton at 273 K and 130 Pa.[12] These data are because krypton has the largest stopping power of these gases. The shape and the intensities of the Cu I spectral image would be explained from the difference in the energy transfer among particles in the plasma plume, between helium, argon, and krypton. Especially in the helium LIP, large parts of energetic particles produced in the breakdown zone might move away without any loss of their kinetic energies due to the small stopping power, leading to no emissions of the Cu I line, as shown in Fig. 2. In contrast, the emission zone of the krypton LIP is concentrated with large emission intensities due to the large stopping power, and the emission zone of the argon LIP is relatively dispersed but has smaller intensities than that of the krypton LIP because the energetic particles have longer lifetime compared to krypton.

Comparison in 2D image between copper and plasma gas emission lines

Figure 3 shows a comparison in 2D emission images between the Cu I 324.75-nm line and the Kr I 431.96-nm line, when krypton gas is introduced at various gas pressures. It is clear to say that the emission zone of the Kr I line is much smaller than that of the Cu I line, regardless of the plasma gas pressure. This effect can be explained by the difference in the excitation energy between the Cu I line (3.82 eV) and the Kr I line (12.78 eV). The excitation to the Kr I line requires larger kinetic energies in the collisional energy transfer, as shown in Eq. (3′), compared to that of the Cu I line; therefore, the emission zone of the Kr I line is restricted adjacently to the breakdown zone where particles having larger kinetic energies still survive. In the result of the argon LIP, the spatial distribution of the Ar I 420.07-nm line (14.50 eV) was similar to that of the Kr I line in the krypton LIP. In the case of the helium LIP, the emission of the He I 388.86-nm line (23.01 eV) was hardly observed in the plasma plume zone, probably because the excitation energy of the He I line was larger. It is interesting to note that the spectrochemical properties of the plasma gas can affect the emission images of the LIP. In fact, the excitation and ionization energies are much different between these plasma gases: for example, the first ionization potential is 24.59 eV for helium, 15.76 eV for argon, and 14.00 eV for krypton.[9–11] We also should consider these spectrochemical parameters in collisional energy-transfer processes occurring in the plasma plume.

Comparison in signal-to-background ratio between plasma gases

For analytical applications in LIPS, we can estimate the optimum position for measuring the emission intensity from the 2D plasma images. The signal-to-background ratio (SBR) is a suitable parameter for the optimization. Figure 4 shows variations in the SBR value of the Cu I 324.75-nm line as a function of the observation height above the sample surface, when krypton (a) or argon (b) was employed as the plasma gas at several different gas pressures. It is clear to say that the breakdown zone just above the surface is not suitable for the observation position due to the smaller SBR, in the argon LIP as well as the krypton LIP. This is because strong emissions from the background appear in this zone. The SBR of the krypton LIP has large values at the height of 1 – 3 mm above the sample surface, which gives slightly different results for the gas pressures, while that of the argon LIP becomes constant values at the height of 0.5 – 4 mm. Concerning the criterion with the SBR value, the krypton LIP is recommended for the analytical applications.

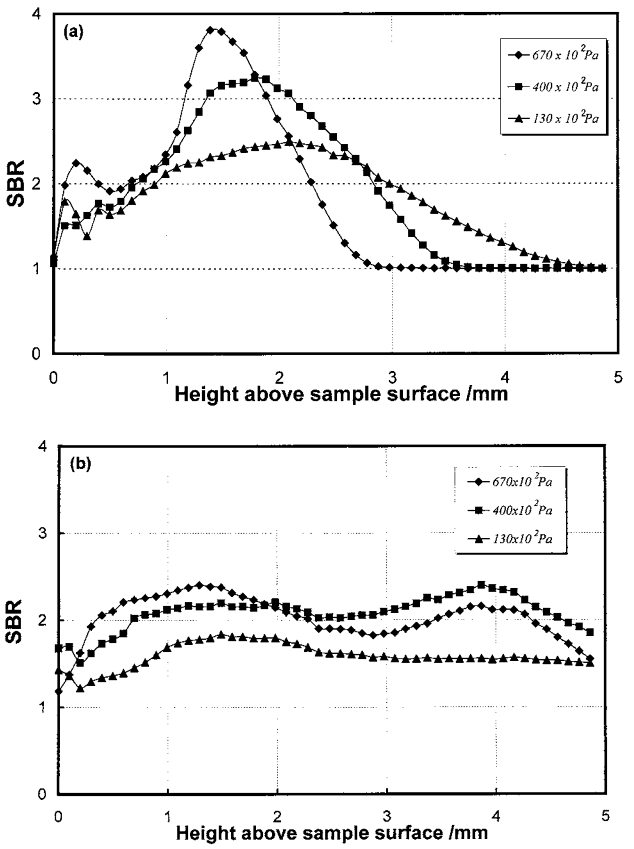

Fig. 4 Variations in the signal-to-background ratio of Cu I 324.75 nm as a function of the height above the sample surface when krypton (a) or argon (b) is introduced at various gas pressures.

Conclusions

The 2D images of emission spectra from laser-induced plasmas, which can be measured by using an imaging spectrograph equipped with a CCD detector, provide useful information on the excitation mechanism as well as on the optimization of experimental parameters for the analytical application. The emission image of the Cu I 324.75-nm line consists of a breakdown spot and a plasma plume where the breakdown zone expands toward the surrounding gas. When krypton, argon, or helium is introduced at various gas pressures, the shape and the intensities of the plasma plume strongly depend on the kind and pressure of the plasma gas. The emission zone of the krypton LIP has the largest intensity, while that of the helium LIP is much less intense, and the zone of the argon LIP expands the most widely. These phenomena can be explained from the difference in the cross-section of collisions between krypton, argon, and helium.

Acknowledgements

The authors gratefully acknowledge financial support by a grant from the Ministry of Environment, Japan. This research is supported also by Grant-in-Aids from the Ministry of Education, Science, Sports and Culture of Japan (No. 18360016).

References

1. J. Sneddon, T. L. Thiem, and Y. I. Lee (ed.), "*Lasers in Analytical Atomic Spectroscopy*", **1997**, VCH Publisher, New York.
2. J. Angeli (ed.), "*Process in Analytical Chemistry in the Steel and Metal Industries*", **2006**, Verlag Glückauf GMBH, Essen.
3. Z. W. Hwang, Y. Y. Teng, K. P. Lee, and J. Sneddon, *Appl. Spectrosc.*, **1991**, *24*, 435.
4. Y. Iida and E. S. Yeung, *Appl. Spectrosc.*, **1994**, *48*, 945.
5. K. Kagawa, K. Kawai, M. Tani, and T. Kobayashi, *Appl. Spectrosc.*, **1994**, *48*, 198.
6. Y. I. Lee, S. P. Sawan, T. L. Thiem, Y. Y. Teng, and J. Sneddon, *Appl. Spectrosc.*, **1992**, *46*, 436.
7. Y. Ushirozawa and K. Wagatsuma, *Spectrosc. Lett.*, **2005**, *28*, 539.
8. Y. Ushirozawa and K. Wagatsuma, *Anal. Sci.*, **2006**, *22*, 1011.
9. C. E. Moore, "*Atomic Energy Levels*", **1947**, Vol. 1, NBS Circular 467, Washington, D.C.
10. C. E. Moore, "*Atomic Energy Levels*", **1952**, Vol. 2, NBS Circular 467, Washington, D.C.
11. C. E. Moore, "*Atomic Energy Levels*", **1958**, Vol. 3, NBS Circular 467, Washington, D.C.
12. A. von Engel, "*Ionized Gases*", **1965**, Clarendon Press, Oxford.